# *Ab-initio* studies on Li doping, Li-pairs, and complexes between Li and intrinsic defects in ZnO

R. Vidya,[1,a)] P. Ravindran,[1,2] and H. Fjellvåg[1]
[1]*Center for Materials Science and Nanotechnology and Department of Chemistry, University of Oslo, Box 1033 Blindern, N-0315 Oslo, Norway*
[2]*Central University of Tamil Nadu, Thanjavur Road, Thiruvarur, 610004 Tamil Nadu, India*

(Received 6 March 2012; accepted 17 May 2012; published online 22 June 2012)

First-principles density functional calculations have been performed on Li-doped ZnO using all-electron projector augmented plane wave method. Li was considered at six different interstitial sites ($Li_i$), including anti-bonding and bond-center sites and also in substitutional sites such as at Zn-site ($Li_{zn}$) and at oxygen site ($Li_o$) in the ZnO matrix. Stability of $Li_{Zn}$ over $Li_i$ is shown to depend on synthetic condition, viz., $Li_{Zn}$ is found to be more stable than $Li_i$ under O-rich conditions. Hybrid density functional calculations performed on $Li_{Zn}$ indicate that it is a deep acceptor with (0/-) transition taking place at 0.74 eV above valence band maximum. The local vibrational frequencies for Li-dopants are calculated and compared with reported values. In addition, we considered the formation of Li-pair complexes and their role on electronic properties of ZnO. Present study suggests that at extreme oxygen-rich synthesis condition, a pair of acceptor type $Li_{Zn}$-complex is found to be stable over the compensating $Li_i + Li_{Zn}$ pair. The stability of complexes formed between Li impurities and various intrinsic defects is also investigated and their role on electronic properties of ZnO has been analyzed. We have shown that a complex between $Li_{Zn}$ and oxygen vacancy has less formation energy and donor-type character and could compensate the holes generated by Li-doping in ZnO. © *2012 American Institute of Physics*. [http://dx.doi.org/10.1063/1.4729774]

## I. INTRODUCTION

Fabrication of optoelectronic devices such as blue and UV lasers and light emitting diodes (LEDs) is one of the most attractive applications of wide-gap semiconductors. ZnO with its wide band gap (3.37 eV at room temperature) and large exciton binding energy (60 meV) has received much attention as a promising material for optoelectronic devices such as LEDs and laser diodes. The possibility of growing many different ZnO nanostructures has opened up a wide range of high technology applications.[1] In addition, among the tetrahedrally bonded semiconductors, ZnO is found to have the highest piezoelectric tensor.[2] This unique combination of piezoelectric, conductive, and optical properties of ZnO made it useful in many devices such as ultrasonic transducers, surface-acoustic-wave devices, and chemical sensors.

A *p-n* homojunction using a wide-gap semiconductor has wide applications such as functional window to transmit visible light and generate electricity in response to the absorption of UV photons. However, unlike the silicon technology it is very difficult to make a *p-n* homojunction using wide-gap semiconductors. It is well known that nominally undoped ZnO exhibits *n*-type conductivity. To realize the optoelectronic devices, an important issue is the fabrication of low-resistance *p*-type ZnO with high hole concentration. However, the realization of low-resistivity *p*-type ZnO has thus far proven difficult due to reasons such as self-compensation, deep acceptor level, and low solubility of the acceptor dopants.

As large number of candidates receive particular attention for introducing *p*-type conductivity in ZnO, the optimal choice of acceptor species remains to be determined. N substituting for O appears promising, while other group-V dopants such as P and As have also been investigated. Unfortunately their acceptor levels are identified to be deep. For example, a recent density-functional study[3] on N-doped ZnO using an accurate hybrid-functional calculation that reproduced experimental band-gap has shown that $N_o$ is in fact a deep acceptor. Moreover Group-V dopants have quite low solubility limits and the reliability of the resulting *p*-type behavior is still the main issue.

Among Group-I elements, Li-doping has received particular attention, mainly because, Li is the most common unintentional dopant in hydrothermally grown ZnO.[4] Recently, *p*-type ZnO was reported to be achievable with Li impurities, although *p*-type conduction is highly sensitive to the growth conditions.[5] Moreover, Li exhibits amphoteric behavior in ZnO, viz., the type of charge carriers generated by Li-doping depends mostly on the site at which Li occupies. For example, if Li occupies an interstitial site it acts as a donor; in contrast, substitutional Li ($Li_{Zn}$) acts as an acceptor. Even though the solubility[6] of Li in ZnO can be up to around 30 at. %, Li doping typically increases the resistivity of *n*-type ZnO leading to semi-insulating samples. Though the increase in electrical resistivity by the introduction of Li ions is detrimental for electrical conductivity, it could be useful for measuring dielectric properties.[7]

a)Electronic address: vidya.ravindran@kjemi.uio.no.

 

Moreover, Li-doping is shown to induce ferroelectric phase suitable for optical memory devices.[8,9] Therefore, understanding the effects of Li doping in ZnO is imminent for device applications. In this work, we have attempted to analyze the effects of Li-doping in ZnO by introducing various defects and defect complexes through super-cell approach and performed structural optimization using accurate density-functional calculations.

Interestingly, Li-doped ZnO has been prepared by many different synthetic techniques and the properties are shown to vary significantly depending on growth conditions. Zeng *et al.*[11] have prepared *p*-type ZnO by mono-doping of Li using dc magnetron sputtering. They have shown that *p*-type conduction is sensitive to the substrate temperature as well as Li-concentration.[12] At 550 °C, more Li atoms substitute for Zn, which act as an effective acceptor and thus the optimized *p*-type conduction is achieved. The acceptable *p*-type conduction identified by room temperature and temperature-dependent Hall-effect measurements was electrically stable over a month. When substrate temperature is reduced to 450 °C, redundant Li atoms are incorporated in the matrix, however the hole concentration is decreased. On the contrary, the ZnO films prepared by pulsed laser deposition (PLD) method showed[14] maximum hole concentration and lowest resistivity at 450 °C. When the substrate temperature is reduced to 400 °C the solubility of Li atoms or $Li_2O$ molecules in ZnO is low and also, when the temperature is increased to 600 °C the amount of Li-acceptor is reduced due to re-evaporation of Li from ZnO lattice. However, Li-doped ZnO thin films prepared by the same PLD method, but epitaxially grown on $LiNbO_3$ substrates, have shown[15] *n*-type conductivity with carrier density of $2.0-3.2 \times 10^{18}\,cm^{-3}$.

Lu *et al.*[5] have prepared Li-doped ZnO by PLD and shown that the type of carrier can be controlled by adjusting the growth conditions. They used an ionization source so that the oxygen chemical potential is increased since excited O radical species are created in an ionized oxygen atmosphere, which provides an oxygen-rich condition for producing ZnO. They have shown that if the ionization source is off, the ZnO films grown in a conventional $O_2$ atmosphere without intentional doping shows *n*-type conductivity. On the other hand, if the ionization source is on, *p*-type conductivity is obtained in undoped ZnO due to the creation of Zn vacancies. Moreover, for ZnO:Li films prepared without using the ionization source the *n*-type conductivity is monotonically reduced when the Li content increases. Further, for ZnO:Li films prepared in the ionized oxygen atmosphere, the *p*-type conductivity is evidently enhanced with the incorporation of Li.

Li-doped ZnO also receives attention as ferroelectric activity was found[11] in Li-doped ZnO, although no phase transition had been reported by Li doping at atmospheric pressure. It is believed that the large difference in ionic radii between the host Zn (0.74 Å) and the dopant Li (0.60 Å) is very important for the appearance of ferroelectricity in Li-doped ZnO.[12] Wang *et al.*[16] have prepared Li-doped ZnO using PLD and measured its ferroelectric and optical properties. They proposed that the off-centered positions of Li substituting Zn atoms lead to ferroelectric distortion. So, it is interesting to study the local structural relaxation by the substitution of Li at the Zn site in ZnO.

Li-doped ZnO thin films were prepared by sol-gel method[7] and the hole concentration was shown to be low at 10 or 12.5 at. % of Li, as holes are compensated by native defects such as $V_o$ and $Zn_i$. However, if 15.0 at. % or more Li atoms entered into the ZnO crystal lattice, Li atoms occupy Zn sites (indicated by the decrease in *c*-axis length). Therefore, stable and optimized *p*-type conduction was obtained by around 15.0 at. % of Li doping. However, on further increase in Li concentration, the electrical conductivity is decreased, may be because some Li atoms do not occupy the Zn site, instead assemble at the crystal grain boundary which could act as a scattering center, thus deteriorating the *p*-type electrical conductivity. Further, Li-doped ZnO powders obtained by ball-milling of $Li_2O$ with ZnO showed increase in electrical conductivity by increase in Li concentration and this is attributed to the possible formation of intrinsic defects such as vacancies.[17] In order to have microscopic understanding about the role of high concentration of Li on electrical conductivity in ZnO detailed electronic structure studies in high concentration of Li-doped ZnO are needed.

A first-principles calculation showed[19] that Li co-doped with cobalt leads to room-temperature ferromagnetism in ZnO which has been confirmed in low-temperature sol-gel synthesized ZnO:Co,Li samples. Recently ferromagnetism in Li-doped ZnO nanorods has been observed[18] with Curie temperature up to 554 K, indicating that it can be a promising dilute magnetic semiconductor useful for spintronic devices.

Lee *et al.*[20,21] proposed a Li-H codoping method for fabricating low-resistivity *p*-type ZnO. They have shown that co-doping H severely suppresses the formation of interstitial donors and the solubility of Li-dopants can be enhanced by the formation of hydrogen-acceptor complexes.[22] However, experimentally it has been shown that 30% of Zn sites can be substituted by Li in single crystals.[8] On the other hand, Wardle *et al.*[23] suggested that *p*-type doping may be limited by the formation of complexes, such as $Li_{Zn}$-$Li_i$ and $Li_{Zn}$-H. So, it is interesting to study the stability and nature of charge carriers of Li-pair complexes in ZnO by *ab-initio* calculation. Li doping was shown[25] to typically increase the resistivity of ZnO which had otherwise very good *n*-type conductivity. Further, it has been theoretically predicted[26] that *p*-type doping in ZnO increases the Madelung energy, which could induce the localization of the acceptor states.[27]

In the present work we report results of accurate total energy calculations based on density functional method by considering Li at substitutional sites ($Li_{Zn}$ and $Li_O$). In addition, we have also considered six different interstitial positions (Fig. 1) in order to find out the most preferable interstitial site for Li in ZnO. The intrinsic defects are known to induce non-stoichiometry in ZnO at ambient conditions. Moreover, in hydrothermally grown ZnO samples, Li concentration of $0.9-1.6\ 10^{17}\,cm^{-3}$ is found,[28] which can account only for 25%–65% of acceptors obtained from Hall measurements and mobility simulations. The remaining acceptors are suggested to have resulted from the co-existence of intrinsic defects and Li-impurities. As defect

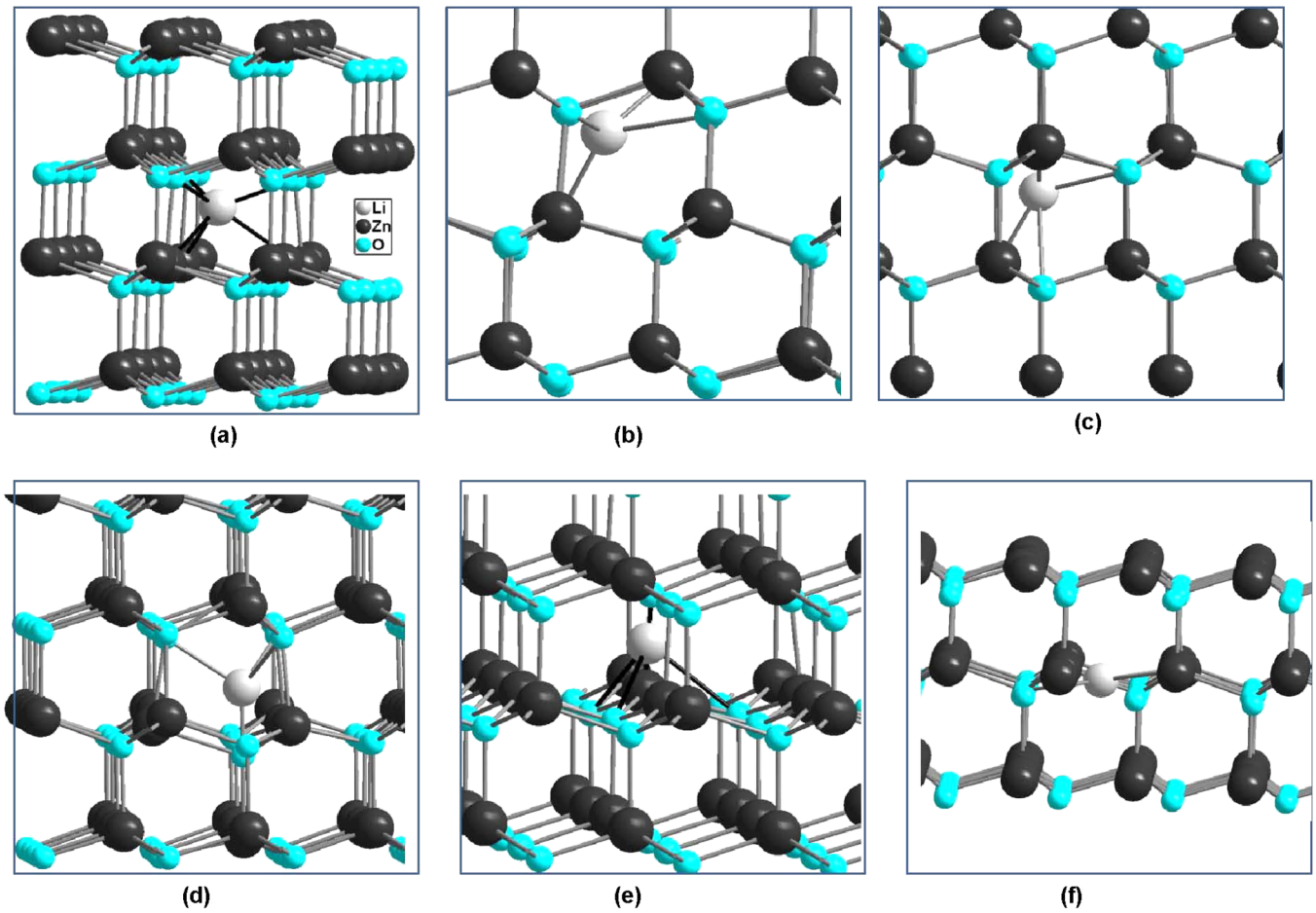


FIG. 1. The different interstitial positions for Li in ZnO (i.e., $Li_i$) considered for the total energy calculations such as (a) $Li_i^{oct}$, (b) $AB_{O,\perp}$, (c) $AB_{Zn,\perp}$, (d) $AB_{O,\parallel}$, (e) $BC_{\parallel}$ (along c-axis), and (f) $BC_{\perp}$ (perpendicular to *c*-axis). The atom labels are given in (a).

complexes formed between intrinsic defects and Li-impurities have received little attention,[23] we have carried out detailed investigation on intrinsic defect complexes with Li impurities and analyzed the energy levels induced by such complexes.

## II. COMPUTATIONAL DETAILS

First-principles calculations have been performed using the projected augmented plane-wave (PAW)[29] method as implemented in the Vienna *ab initio* simulation package (VASP).[30] We have performed calculations for supercells with 192 and 256 atoms. The defects are simulated by adding and/or removing constituent atoms to/from the supercell. As the calculated formation energy does not vary very much for 192 and 256 atoms supercells, we used the 192 atom supercells for simulating defect complexes. We have tested the total energy convergence with respect to **k**-points and plane wave energy cutoff. For the sake of more accurate results we used plane-wave energy cutoff of 550 eV. Brillouin zone sampling was done in the Monkhorst-Pack scheme with **k**-point mesh of $2 \times 2 \times 2$ for supercells with 192 atoms. The optimization of the atomic geometry was performed via a conjugate-gradient minimization of the total energy, using Hellmann-Feynman forces on the atoms and the stresses in the unit cell. During the simulations, atomic coordinates and axial ratios were allowed to relax for different volumes of the unit cell. Convergence minimum with respect to atomic relaxations was attained when the energy difference between two successive iterations was less than $10^{-6}$ eV per unit cell and the forces acting on the atoms were less than 1 meV $Å^{-1}$. For charged defects a jellium background charge was used. Exchange and correlation effects are treated under the generalized-gradient-approximation (GGA)[31] including the Perdew-Burke-Ehrenkof (PBE) functional.

The defect formation energy is calculated as described in Refs. 33–35. We have calculated the formation energy of Li-based defects by deriving chemical potential of Li from metallic Li. The formation energy derived from chemical potential of Li from $Li_2O$ and $Li_2O_2$ is 3.14 and 3.46 eV higher in energy, respectively.

The dipole correction to the formation energy is included by calculating the correction terms for 72 and 192 atom supercells. These values are extrapolated to infinity with respect to 1/L where L is the linear length of the supercell. It is well known that present type of density-functional calculations underestimate the band-gap significantly and therefore many correction schemes are adapted depending upon the type of the defect. One of the common correction methods is to perform scissor operation which shifts

theoretical conduction band minimum (CBM) to match with the experimental band-gap value. As the density-functional theory (DFT)-based calculations severely underestimate band-gap [$E_g$; that obtained by GGA is 0.88 eV], the transition levels are shown with respect to corrected $E_g$ values. The correction has been carried out by performing GGA + $U$ calculation that provided an $E_g$ of 1.84 eV with the valence band maximum (VBM) pushed downwards. Then, a scissor operation was performed to push the CBM upwards to match with the experimental value. In order to find out the defect level induced by $Li_{Zn}$ which is a polaranic defect, we have performed structure optimization and electronic structure calculation using the Heyd-Scuseria-Ernzerhof (HSE) hybrid functional[32] in neutral and 1− charge states. A screening parameter of $a = 0.375$ was used which reproduced experimental parameters for ZnO and provided a band-gap of 3.34 eV.

Moreover, we have calculated binding energy of a defect-complex (AB) formed between individual defects A and B using the following convention: Binding energy $E^b(AB) = E^f(A) + E^f(B) - E^f(AB)$, where $E^f(A)$, $E^f(B)$, and $E^f(AB)$ are formation energy of defect A, defect B, and defect-complex AB, respectively. Therefore, a positive binding energy represents a bound system.

In order to identify point defects experimentally, vibrational modes are often used to characterize various defects. Therefore, we have calculated the vibrational modes by obtaining second-derivative of the total energy with respect to displacement. The phonon frequencies are derived from "frozen-phonon" calculations, i.e., distortions consistent with the symmetry of the mode are introduced and the corresponding total energy is calculated. In the present computations, the second derivatives required for the force-constant matrix elements were obtained by calculating the forces exerted on all atoms when one or two of the atoms are displaced in the $a$, $c$ direction. Both positive and negative displacements were considered to take into account possible anharmonic effects. For all the frozen-phonon calculations, we have used respective supercells (with 192 atoms). The coefficient $a2$ in the second-order term in the following equation is the harmonic contribution to the total energy, naturally referred to as a force constant. Knowing this, we then obtain the phonon frequency $\nu$ as

$$\nu = (2\pi L)^{-1}\left[\frac{a2}{2\mu}\right]^{1/2}, \quad (1)$$

where $\mu$ is the mass of the atom which is involved in a given phonon mode. From the second derivative of the total energy or the first derivative of the force with respect to the displacement of respective atom, we have calculated the A1 and E phonon frequencies. More details of these calculations are given elsewhere.[36]

## III. RESULTS AND DISCUSSION

### A. Li at interstitial sites

Many different interstitial sites for H at ZnO matrix have been discussed in the literature,[37] viz., different antibonding and bond-center sites. Similar to the H case, we have considered Li at six different interstitial sites in ZnO as shown in Fig. 1.

Among these interstitial sites considered (as seen from Table I), Li prefers to occupy the octahedral interstitial site ($Li_i^{oct}$) at which it forms six bonds with neighboring atoms (three Li-O bonds have 2.14 Å and three Zn-O bonds have 2.30 Å bond-lengths). Upon relaxation, this atom has displaced 0.1 Å closer to O atoms and 0.27 Å away from Zn atoms. Moreover, this $Li_i^{oct}$ atom does not influence displacement of neighboring host atoms from their equilibrium positions. This could explain why this site configuration has lower formation energy compared to other configurations considered. The next higher energy $Li_i$ ($AB_{Zn,\perp}$) site is a distorted tetrahedral site at which Li forms 3 bonds with O atoms (with lengths ranging from 1.79 to 2.35 Å) and 1 bond with a Zn atom at a distance of 2.32 Å). The occupation of Li at $Li_i$ ($AB_{Zn,\perp}$) site displaced neighboring Zn atom from its equilibrium position. Similarly, the Li at $AB_{O,\parallel}$ position also influences displacements of neighboring oxygen atoms from their equilibrium positions. This interstitial Li atom also forms distorted tetrahedral site with one oxygen atom at 1.62 Å and remaining three O atoms at a distance of 2.15 Å. However, unlike H interstitial, $Li_i$ does not prefer to take up the bond-center positions ($BC_\parallel$ and $BC_\perp$) and this may be due to considerably larger covalent radii of Li (1.28 Å) compared with that for H (0.38 Å).

It may be noted that the formation of $Li_i$ is independent of Zn or O partial pressures. As seen from Tables I, the 1 + charge state (donor) of $Li_i$ is lower in energy than neutral state for all interstitial positions considered, except for $BC_\perp$ position. The acceptor-type charge state (1−) is approximately 0.30 eV higher in energy than the neutral state. However, for the $BC_\perp$ position the donor-type state is 2.55 eV higher in energy than the neutral state. If the calculations are

TABLE I. Energy of formation of $Li_i$ in different possible interstitial sites (notations are as given in Fig. 1). The Li chemical potential is derived from metallic Li. The values correspond to the Fermi energy at valence band maximum.

| Defect | Charge state | Formation energy (eV) |
|---|---|---|
| $Li_i^{oct}$ | 0 | 5.70 |
| | 1+ | 4.67 |
| | 1− | 5.98 |
| $Li_i$ ($AB_{Zn,\perp}$) | 0 | 6.18 |
| | 1+ | 5.50 |
| | 1− | 6.78 |
| $Li_i$ ($AB_{O,\parallel}$) | 0 | 6.72 |
| | 1+ | 6.02 |
| | 1− | 7.30 |
| $Li_i$ ($AB_{O,\perp}$) | 0 | 15.89 |
| | 1+ | 14.99 |
| | 1− | 16.91 |
| $Li_i$ ($BC_\perp$) | 0 | 14.34 |
| | 1+ | 16.89 |
| | 1− | 11.58 |
| $Li_i$ ($BC_\parallel$) | 0 | 31.82 |
| | 1+ | 31.30 |
| | 1− | 32.15 |

performed with constraining Li to be at the $BC_{\perp}$ position, the host atoms up to third nearest-neighbor positions undergo significant displacements from their equilibrium positions and occupy the interstitial sites. Therefore, even if $Li_i^{1-}$ state is achieved by placing Li at $BC_{\perp}$ position by some means, the crystal structure would not be stable. This implies that Li atom occupying an interstitial site can never have an acceptor-type character.

$Li_i^{oct}$ is a shallow donor, in agreement with previous theoretical studies.[20,23] As a shallow donor level is introduced below CBM by $Li_i$, it can be taken as an indication of decrease in $E_g$, in good agreement with the reduction in $E_g$ (from 3.37 eV to 3.25 eV) observed by absorption band-edge from optical measurements.[7] Moreover, photoluminescence (PL) spectra shows[47] an emission band at 0.15 eV below $E_g$ (at 3.15 eV). (However, it may be noted that the concentration of Li in our simulation is significantly lower than that in experimental observations).

Density of states (DOS) analysis shows that $Li_i^{1+}$ *s*-states are more prevalent in conduction band than in valence band, as expected and are energetically well dispersed. A real-space first-principles calculation[48] also found that the defect wave function arising from $Li_i^{oct}$ is not spatially bound to the defect atom. The hyperfine splittings of $^7$Li in Li-doped ZnO nanoparticles are measured[49,50] to be much smaller than that for atomic Li, indicating that defect levels introduced are shallow and weakly bound. This is consistent with the present observation of formation of shallow donor by $Li_i^{oct}$ in ZnO.

The energetically well dispersed $Li_i^{1+}$ *s*-orbital DOS could also explain why $Li_i$ donor-type character (i.e., *n*-type conductivity) is more dominant than the $Li_{Zn}$ acceptor-type character in ZnO. As at CBM (*n*-type condition) the acceptor-type $Li_{Zn}$ is having lower energy than the donor-type $Li_i$, the holes would compensate the electrons generated by donor-type defects which may explain the reason for increase in resistivity[25] at *n*-type condition due to Li-doping.

### B. Role of Li substitution at Zn ($Li_{Zn}$) and oxygen ($Li_O$) sites

As the formation of Li at Zn and O sites requires formation of Zn-vacancy($V_{Zn}$) and Oxygen-vacancy ($V_O$), respectively, they depend on the oxygen partial pressure. Between extreme Zn-rich and O-rich conditions, the oxygen chemical potential varies by 3.38 eV. This variation is given as percentage of O-partial pressure in Fig. 2. As can be seen, $Li_i$ is the predominant defect under Zn-rich condition. It can be noted that under O-rich condition the formation energy of $Li_{Zn}$ is very much lower than that of $Li_i$ at Zn-rich condition. Therefore, $Li_{Zn}$ readily forms under O-rich condition, especially above 62%–64% of oxygen partial pressure. Below that value and under equilibrium condition, $Li_i$ is the dominant defect. Especially $Li_i$ has ca. 0.5 eV lower formation energy than $Li_{Zn}$ from $Li_2O$ which is the most common Li source. $Li_O$ is in a donor state (1+ state is 1.98 eV lower in energy than neutral state) and it has higher formation energy under both Zn-rich and O-rich conditions as well as at equilibrium. Hence, $Li_O$ is not a stable defect and we have not considered it for further discussions.

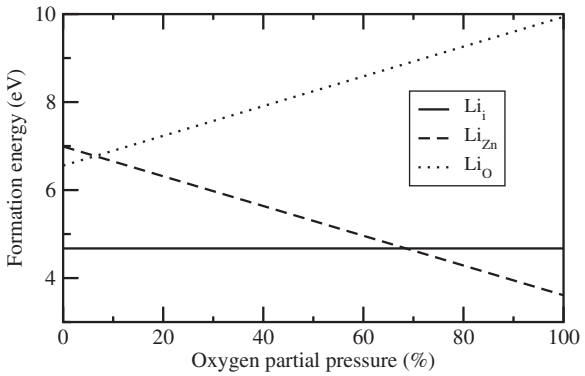


FIG. 2. Formation Energy of $Li_i^{oct}$, $Li_{Zn}$, and $Li_O$ calculated as a function of oxygen partial pressure. Zn-rich condition corresponds to 0% and Oxygen-rich to 100% of Oxygen partial pressure. Chemical potential of Li is from metallic Li.

The $Li_{Zn}$ defect has ca. 0.2 eV lower formation energy for acceptor (1−) state than the neutral state. Our structural relaxation shows that if $Li_i$ is placed in the vicinity of a $V_{Zn}$ it relaxes down to the $V_{Zn}$ site. This indicates that $Li_{Zn}$ can be stabilized in ZnO if one could dope Li in ZnO samples that contain $V_{Zn}$. Our previous work[35] and other theoretical studies[45,46] have shown that $V_{Zn}$ is the dominant defect under O-rich condition. The present observation of the formation of acceptor states by $Li_{Zn}$ is consistent with experimental results from Lu *et al.*[5] who showed that, upon using ionizing oxygen gas which increases oxygen chemical pressure, the *p*-type conductivity in ZnO is enhanced with the incorporation of Li at the Zn vacancy sites. For ZnO:Li films prepared without using the ionization source, a sharp decrease in electron concentration was observed as compared with the undoped ZnO film. The *n*-type conductivity is monotonically reduced as the Li content increases, demonstrating that Li compensates electrons in ZnO. Moreover, it may be noted that ZnO samples have Zn-terminated face (with negative surface polarity) and O-terminated face (with positive surface polarity). When the Li-doped ZnO sample is heat treated in air, the concentration of $V_{Zn}$ at the O-face is increased because of low Zn partial pressure. Therefore, transport of $Li_{Zn}^{1-}$ acceptors towards the oxygen face is enhanced during the heat treatment.[4,38]

$Li_{Zn}$ receives particular attention not only for *p*-type conductivity but also for ferroelectricity. Experimental studies[8,10–12] suggest that ZnO exhibits ferroelectricity when Li occupies the Zn site, owing to the mismatch between their ionic radii. The interatomic distance between Zn and O in pure ZnO is 2.005 Å and 2.014 Å along *ab* plane and along *c*-axis, respectively. The corresponding distances for Li-O is 2.015 Å and 2.023 Å, respectively.

According to our calculations based on PBE functional, $Li_{Zn}^{1-}$ states occur at the top of VBM, indicating that it is a shallow acceptor, in agreement with previous studies.[22–24] If the Madelung correction of 0.251 eV is included, the (0/1-) transition is found to take place at 0.05 eV above VBM. A study based on ultra-soft psuedopotentials has also found[24] localized peak close to VBM which has been assigned to Li 2*s* and 2*p* orbitals.

However, recent calculations based on more accurate methodology[40] and hybrid-functional calculations have

TABLE II. Local vibrational frequencies (in $cm^{-1}$) of Li-impurities in ZnO.

| Defect | Mode | Frequency | |
|---|---|---|---|
| | | $^6$Li | $^7$Li |
| $Li_i^{oct}$ | $A_1$ (along $c$) | 349.3 | 323.4 |
| | $E$ ($\perp$ to $c$) | 445.5 | 412.5 |
| $Li_{Zn}$ | $A_1$ (along $c$) | 373.1 | 345.5 |
| | $E$ ($\perp$ to $c$) | 365.9 | 338.8 |

shown[41,42] $Li_{Zn}$ to be a deep acceptor. In order to find out the (0/-) transition level of $Li_{Zn}$ accurately, we have performed complete structural relaxation using hybrid (HSE) functionals as implemented in the VASP program for a 72-atom supercell. In contrast to the PBE calculations, the Li-O distances for $Li_{Zn}$ are reduced by 2.14% and 2.53% along *ab* plane and *c*-axis, respectively. All the four O atoms surrounding the $Li_{Zn}$ have a uniform bond-length of 1.961 Å. Moreover, the Li atom is slightly displaced from its initial position and moved towards the axial O atom along *c*-axis, could be due to the localization of hole at the axial O atom.[40–42] It may be noted that a decrease in *c*-axis length by Li-doping is also put forth by experimental studies. For example, a slight change is lattice parameters are observed in Li-doped ZnO thin films for Li content of 4 at. %.[13] Our HSE calculations provide the (0/-) transition level of $Li_{Zn}$ to be at 0.743 eV above VBM, in good agreement with experimental value of 0.8 eV,[43] implying that $Li_{Zn}$ is a deep acceptor. A recent electron paramagnetic resonance and PL spectroscopy study[44] on Li-doped ZnO nanocrystals has also identified Li acceptor with an acceptor energy of 0.8 eV.

As described in Sec. II, the local vibrational (LV) mode frequencies for Li are calculated and shown in Table II, are in good agreement with earlier theoretical values.[23] As experimental determination of these frequencies involves Li-isotopes, the isotopic mass is taken into account in the present calculation. The LV frequencies for $Li_i^{oct}$ indicate significant difference in the bond strengths between bonds along *c* and perpendicular to *c*-axis. In contrast, the $Li_{Zn}$ bonds have similar strengths along *c*-axis and perpendicular to the *c*-axis. The Raman spectra measured for Li-doped ZnO thin films show two peaks at 438 and 579 $cm^{-1}$ assigned to the longitudinal vibration modes E2 and E1, respectively.[39] Moreover, the Li-doped films exhibited high conductivity. Therefore, the experimentally observed E2 peak can be attributed to $Li_i$ which acts as a donor and expected to increase conductivity.

### C. Li-pair complexes

Many studies have found that the *p*-type conductivity decreases when the concentration of Li increases in ZnO. As the probability to form Li-pairs is more by increasing the concentration of Li doping in ZnO, we have carried out calculations for pairs of $Li_i$, $Li_{Zn}$, and $Li_i + Li_{Zn}$ (Fig. 3) to understand their stability and role in the electronic properties in ZnO. For the case of $Li_i$ pair, one Li is placed at the octahedral interstitial and another at $AB_{Zn,\perp}$, as this interstitial site is next higher in energy. We found that the formation

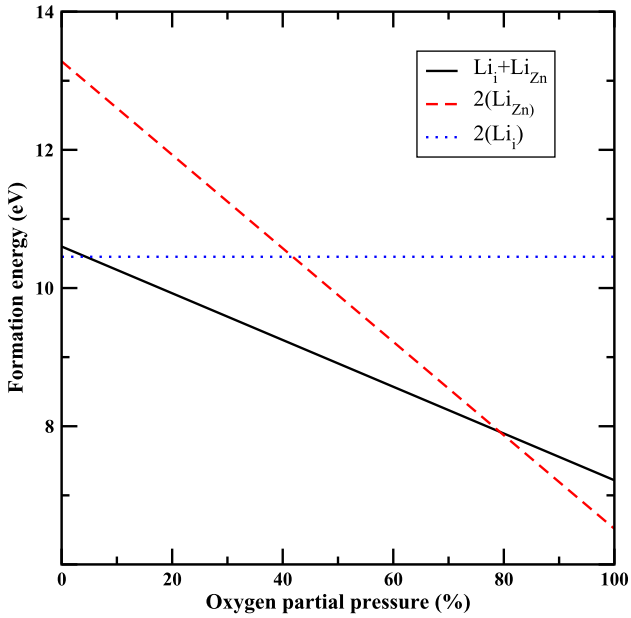


FIG. 3. Formation energy of Li-pair complexes as a function of oxygen partial pressure; Zn-rich (0%) O-rich (100%).

energy is 5.68 eV for the neutral state and as expected, the double donor state is 2.20 eV lower in energy (the values are calculated from chemical potential of metallic Li).

When $Li_2O$ is used as the source for Li, and under O-rich condition, $Li_{Zn}$ pairs are more probable to form according to the following equation:

$$Li_2O + 2V_{Zn} \rightarrow 2Li_{Zn}^{-} + O^0 + 2h. \quad (2)$$

The formation of $Li_{Zn}$-pair requires 7.02 eV/pair in Zn-rich condition and only 0.26 eV/pair under O-rich condition. The 2– charge state is found to be 0.12 eV/pair lower in energy than the neutral state. As $V_{Zn}$ is less probable to form under Zn-rich condition, the formation of $Li_{Zn}$ pair under this condition requires a large energy. This pair has a binding energy of 5.58 eV. Similar to the case of single $Li_{Zn}$ defect the PBE functional shows that the $Li_{Zn}$ pair is also a shallow acceptor, with 2- to 0 transition taking place exactly at the VBM. This suggests that p-type conductivity in ZnO can be induced, if the ZnO samples are prepared in oxygen-rich condition with high concentration of Li, i.e., by introducing $Li_{Zn}$-pairs. In order to find out the position of defect level induced by the $Li_{Zn}$-pair more accurately, computationally demanding HSE functional-based calculations are required.

To understand the interaction between Li at the interstitial and substitutional positions in ZnO we have also investigated the $(Li_i + Li_{Zn})$ pair complex. As we have shown that the $Li_i^{oct}$ has the lowest formation energy than Li at other interstitial positions, we have simulated the $(Li_i^{oct} + Li_{Zn})$ pair by placing a Li atom at $Li_i^{oct}$ and another Li at Zn site at a distance of 2.306 Å and made complete structural relaxation. The formation energy of $(Li_i + Li_{Zn})$ is 4.34 eV/pair and 0.96 eV/pair under Zn-rich and O-rich conditions, respectively. Interestingly, the neutral state is 0.687 eV lower in energy than the 1 – state. Therefore, this pair could compensate charges on increasing the Li-content as suggested

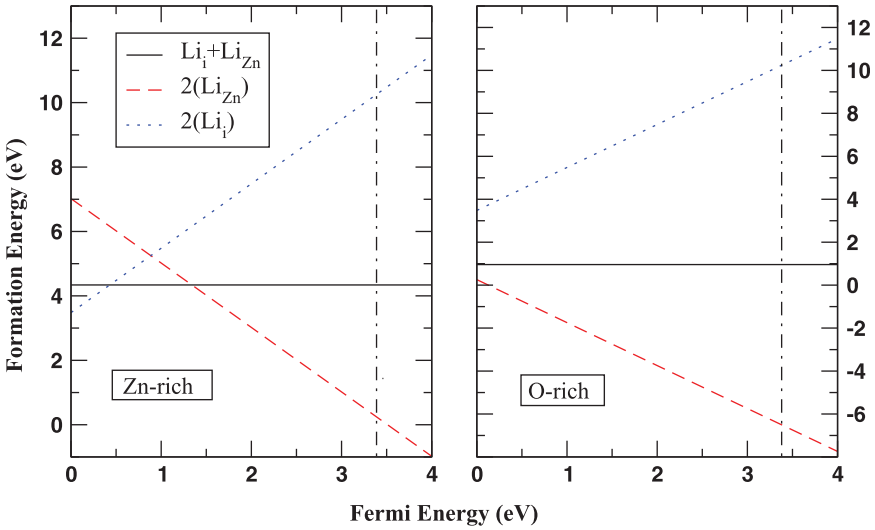


FIG. 4. The formation energy of Li-pair complexes as a function of Fermi energy under Zn-rich and O-rich conditions.

earlier.[23] Moreover, the binding energy for $Li_i + Li_{Zn}$ pair is also more (7.13 eV) compared to other Li-pairs indicating that this pair is more stable. It may be noted that, though $Li_i + Li_{Zn}$ pair is more probable to form in ZnO, it will not contribute to the electrical conductivity owing to the fact that neutral state is more stable for this defect.

As seen from Fig. 3, the double-donor $Li_i$-pair is stable in a narrow window under extremely Zn-rich conditions. On the other hand, the double-acceptor $Li_{Zn}$ is stable above 80% of oxygen partial pressure. The compensating $(Li_i + Li_{Zn})$ pair is stable for most of the growth conditions as well as at equilibrium conditions. Under equilibrium condition, the compensating $(Li_i + Li_{Zn})$ pair is ca. 1 eV/pair lower in energy than the double acceptor $2Li_{Zn}$. However, under extreme O-rich condition and upto 80% of oxygen partial pressure, $2Li_{Zn}$ becomes stable. Therefore, if one could produce Li-doped ZnO at O-rich condition, the *p*-type conductivity can probably be achieved even for higher concentrations of Li. The above discussion corresponds to the Fermi energy ($E_F$) at the VBM which can provide a clue for synthesizing Li-doped ZnO.

As the energetics can become different for $E_F$ values greater than VBM, the formation energy of Li-pair complexes under Zn-rich and O-rich conditions are shown as a function of $E_F$ in Fig. 4. Under extreme Zn-rich condition, the double donor $Li_i$ pair is stable up to $E_F = \text{VBM} + 0.5$ eV. Then, the compensating $(Li_i + Li_{Zn})$ becomes stable for $E_F$ up to 1.5 eV. The double acceptor $Li_{Zn}$ pair is stable for the remaining $E_F$ values and this could explain the increase in resistivity as the Li concentration increases in some samples since these acceptors will compensate the donors created by other defects. Unlike the Zn-rich situation, if Li-doping is carried out under O-rich condition, the double acceptor $2Li_{Zn}$ is stable for all $E_F$ values from VBM to CBM. When a single Li atom occupies Zn-site ($Li_{Zn}$) in ZnO lattice, the $E_F$ is pinned at 2.2 eV and 0.48 eV at Zn-rich and O-rich conditions, respectively, due to self-compensation. However, Fig. 4(b) clearly shows that the self-compensation can be avoided if a $2Li_{Zn}$ is created under extreme O-rich synthetic condition. However, whether $2Li_{Zn}$ leads to *p*-type conductivity in ZnO can be ascertained only from accurate HSE-based hybrid functional calculations.

### D. Complexes between $Li_i$ and intrinsic defects

Experimental studies based on Secondary Ion Mass Spectroscopy (SIMS) profiling, scanning spreading resistance measurements, and positron annihilation spectroscopy indicated that Li impurities are electrically passivated through trapping by vacancy clusters which are generated by ion implantation and subsequent flash annealing.[4] Moreover, in a Li-doped ZnO thin film prepared by sol-gel method, a peak centered at 385 nm in PL spectra is assigned to Li-acceptor-bound-exciton.[7] The monovalent Li ions can create some compensating oxygen vacancies in the ZnO lattice. Further, if the most common source of Li ($Li_2O$) is used to dope Li into ZnO, some intrinsic defect formation is possible based on the following equations:

$$Li_2O \rightarrow 2Li_{Zn}^{1-} + O_O^0 + V_O^{2+}, \tag{3}$$

$$Li_2O + O_i^{2+} \rightarrow 2Li_{Zn}^{1-} + 2O_O^0, \tag{4}$$

$$Li_2O \rightarrow 2Li_i^{1+} + O_i^{2-}, \tag{5}$$

$$Li_2O \rightarrow Li_{Zn}^{1-} + Li_i^{1+} + O_O^0. \tag{6}$$

Therefore, we have modelled Li-impurities together with some of the predominant intrinsic defects under Zn-rich as well as at O-rich conditions. The $Li_i$-intrinsic defects complex formation energy is given in Table III. The formation energy of $Li_i$ depends on the Li-chemical potential involved during the Li doping process. Moreover, the formation of intrinsic defects depends on the Zn and O chemical potentials. Therefore formation energy of complexes is given at Zn-rich and O-rich conditions. From Table III, it is clear that the complexes between $Li_i$ and the dominant intrinsic defects (viz., $V_O$, $Zn_i$, and $Zn_O$) at Zn-rich conditions have lower formation energies. As these defects are stable at 2+ charge state, their complexes with $Li_i$ have lower energy at 3+ charge state. Among these defect complexes $(Li_i + V_O)$ has negative binding energy, indicating the instability of this complex. The $(Li_i + Zn_O)^{3+}$ complex has the lowest formation energy and highest binding energy at Zn-rich condition.

TABLE III. The calculated formation energies of defect complexes between $Li_i$ and intrinsic defects. The Li chemical potential is derived from metallic Li. The formation energy estimated from the chemical potential of $Li_2O$ and $Li_2O_2$ is 3.14 and 3.46 eV higher in energy, respectively. The values correspond to the Fermi energy at valence band maximum. The values in brackets are binding energy of the defect complexes in eV.

| | | Formation energy (eV) | |
|---|---|---|---|
| Defect complex | Charge state | Zn-rich | O-rich |
| $Li_i + V_O$ | 0 | 6.24 | 9.62 |
| | 1+ | 5.25 (−1.77) | 8.64 |
| | 3+ | 5.26 | 8.64 |
| $Li_i + Zn_i$ | 0 | 8.59 | 11.97 |
| | 1+ | 6.44 | 9.83 |
| | 2+ | 5.82 | 9.20 |
| | 3+ | 5.14 (0.14) | 8.52 |
| $Li_i + Zn_O$ | 0 | 8.43 | 15.20 |
| | 1+ | 6.39 | 13.15 |
| | 2+ | 5.58 | 12.35 |
| | 3+ | 4.71 (0.49) | 11.47 |
| $Li_i + V_{Zn}$ | 0 | 8.98 | 5.59 |
| | 1+ | 9.02 | 5.64 |
| | 1− | 8.94 | 5.56 (0.94) |
| $Li_i + O_i$ | 0 | 10.65 | 7.23 |
| | 1+ | 9.00 | 5.62 (2.91) |
| | 2+ | 9.02 | 5.63 |
| $Li_i + O_{Zn}$ | 0 | 20.84 | 14.07 |
| | 1+ | 20.82 | 14.06 |

Since the doubly ionized $Zn_i$ has delocalized electrons at the CBM, charge can be transferred from $Zn_i$ to the empty $Li_i^{1+}$ states similar to the case with $Co + Zn_i$ complex in Co-doped ZnO.[51] As noted in our previous work,[35] $O_i$ has lower energy under neutral state at O-rich condition. Therefore, $(Li_i + O_i)^{1+}$ complex has dominant donor character. As mentioned earlier $Li_i$ will relax down to $V_{Zn}$ if kept closer and unconstrained. Therefore, the $(Li_i + V_{Zn})$ is modelled by performing constrained calculations. Even though 1− state of $(Li_i + V_{Zn})$ complex has lower energy of formation, the binding energy of this complex is small compared to that of the donor-type $(Li_i + O_i)$ complex.

In order to understand the behavior of defect complexes under *p*-type(at VBM) and *n*-type (at CBM) conditions and charge transitions caused by defect complexes, the formation energy of more dominant complexes is shown as a function of Fermi energy under Zn-rich and O-rich conditions in Figs. 5(a) and 5(b). If one compares the stability of $Li_i +$ intrinsic defect complexes under Zn-rich condition, the donor type complexes such as $Li_i + Zn_i$ and $Li_i + Zn_O$ are stable at VBM and up to $E_F$ values of 1.2 eV. For the higher $E_F$ values, the acceptor-type $Li_i + V_{Zn}$ becomes the dominant defect complex. On the other hand, under O-rich condition, the acceptor-type $(Li_i + V_{Zn})$ complex is stable for the entire $E_F$ range.

### E. Complexes between $Li_{Zn}$ and intrinsic defects

We have shown in Sec. III B that $Li_{Zn}$ has the possibility of stabilization in a narrow window of higher oxygen partial pressure. Therefore, formation of complexes of $Li_{Zn}$ with native defects is studied and the formation energies are given in Table IV. Even though the $(Li_{Zn} + O_i)$ has the highest binding energy under O-rich condition, it has higher formation energy than the donor-type $(Li_{Zn} + V_O)$ complex. Moreover, the acceptor-type $(Li_{Zn} + V_{Zn})$ has very little binding energy in spite of having almost the same formation energy as that of $(Li_{Zn} + V_O)$. The formation of the donor-type $(Li_{Zn} + V_O)$ complex may compensate the few holes generated by $Li_{Zn}$ at O-rich condition and this could also explain the difficulty in obtaining *p*-type conductivity.

Formation energy of complexes between $Li_{Zn}$ and intrinsic defects as a function of $E_F$ is given in Fig. 6. The present study suggests that, under Zn-rich condition, donor-type defects are predominant. Even for $Li_{Zn}$ which has acceptor character, when it forms complexes with donor defects such as $V_O$, $Zn_i$, and $Zn_O$, the donor character becomes predominant. The defect complexes such as $(Li_i + Zn_O)$ and $(Li_{Zn} + Zn_O)$ are found to be shallow donors, similar to native $Zn_O$ defect. As shown before[35] the $V_O^{2+}$ has defect levels deep inside $E_g$ and this defect forms a complex with $Li_{Zn}$ gives rise to the $1+ \rightarrow 0$ transition of $Li_{Zn} + V_O$ deep inside the band-gap. In contrast to Zn-rich condition, under O-rich condition, the acceptor-type defects are more predominant.

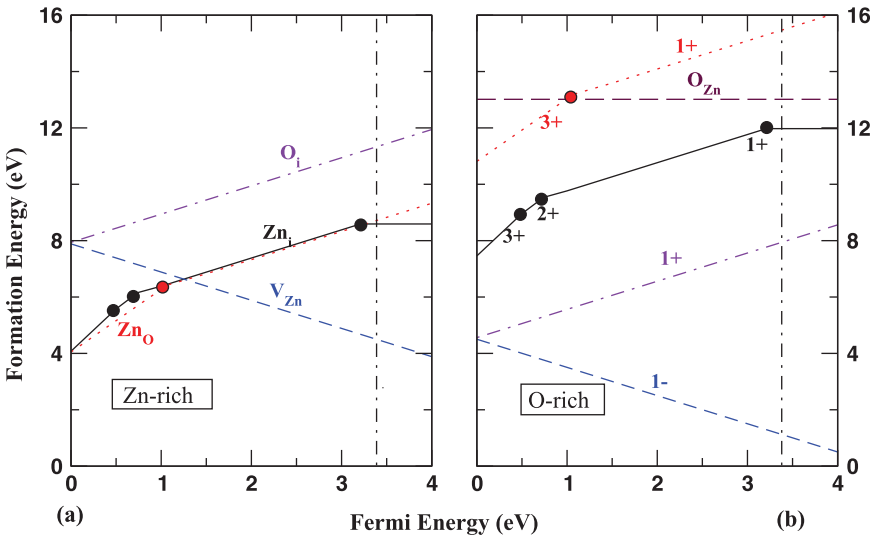


FIG. 5. Formation energy of defect complexes formed between $Li_i$ and intrinsic defects under (a) Zn-rich and (b) O-rich conditions. The dots indicate charge-transition points and the charge states are given on the illustration.

TABLE IV. Formation energies of defect complexes between $Li_{Zn}$ and intrinsic defects. The Li chemical potential is derived from metallic Li. The formation energies derived from chemical potential of $Li_2O$ and $Li_2O_2$ are 3.14 and 3.46 eV higher in energy, respectively. The values listed are corresponding to the Fermi energy at valence band maximum. The values in brackets are binding energy in eV.

| | | Formation energy (eV) | |
|---|---|---|---|
| Defect complex | Charge state | Zn-rich | O-rich |
| $Li_{Zn}+V_O$ | 0 | 5.98 | 5.98 |
| | 1+ | 5.34 | 5.34 (0.33) |
| | 3+ | 5.45 | 5.45 |
| $Li_{Zn}+Zn_i$ | 0 | 7.26 | 7.26 |
| | 1+ | 6.57 | 6.57 (0.90) |
| | 2+ | 6.59 | 6.59 |
| $Li_{Zn}+Zn_O$ | 0 | 7.00 | 10.38 |
| | 1+ | 6.17 (1.16) | 9.55 |
| | 2+ | 6.45 | 9.83 |
| $Li_{Zn}+V_{Zn}$ | 0 | 12.23 | 5.47 |
| | 1− | 12.13 | 5.37 |
| | 2− | 12.07 | 5.30 (0.01) |
| $Li_{Zn}+O_i$ | 0 | 13.02 | 6.26 |
| | 1+ | 13.06 | 6.29 |
| | 1− | 12.99 | 6.23 (5.85) |
| $Li_{Zn}+O_{Zn}$ | 0 | 17.03 | 6.89 |
| | 1− | 17.46 | 7.31 |
| | 2− | 18.09 | 7.94 |

However, at VBM the acceptor-type ($Li_{Zn}+V_{Zn}$) and donor-type ($Li_{Zn}+V_O$) have almost the same energy of formation indicating that the probability of compensating the holes created by ($Li_{Zn}+V_{Zn}$) is high. The *p*-type doping using Li species causes a remarkable increase in the Madelung energy,[52] resulting in the instability of ionic charge distributions in ZnO: Li. Therefore, the formation of $V_O$ in the vicinity of the impurity $Li_{Zn}$ sites is energetically favorable in ZnO: Li. This means that the doping of Li gives rise to bad crystallinity due to the compensation by $V_O$. As a result, ZnO: Li crystals or thin films probably exhibit high resistivity by increase of electron scattering by poor crystallinity. The ($Li_{Zn}+Zn_i$) complex also has donor-type character with binding energy of 0.90 eV which is found to be consistent with the calculated value of 1.09 eV reported earlier.[53]

The ($Li_{Zn}+V_{Zn}$) complex in 2− charge state is having lower energy than the ($Li_i+Li_{Zn}$) under the O-rich condition. Unfortunately, the ($Li_{Zn}+V_O$) in donor state is very much lower in energy than the double acceptor ($Li_{Zn}+V_{Zn}$). As $V_{Zn}$ and $V_O$ are involved in the ($Li_{Zn}+V_O$) complex, its formation energy is independent of oxygen chemical potential. The results from our structural optimization indicate that the reduction in *c*-axis of Li-doped samples may not be attributed to the single $Li_{Zn}$ defect. We have shown earlier[37] that a single $V_O^{2+}$ actually reduces volume by 0.4%. As the $Li_{Zn}+V_O$ has lower formation energy than $Li_{Zn}$, the decrease in *c*-axis length can be attributed to this defect complex. However, it may be noted that the complexes formed between $Li_{Zn}$ with $V_O$ and $V_{Zn}$ have very small binding energy compared to that of the compensating ($Li_i+Li_{Zn}$) complex.

## IV. SUMMARY

We have performed density-functional calculations for Li-doped ZnO using large supercells. Among the octahedral, anti-bonding, and bond-centered interstitial positions considered, Li at the octahedral ($Li_i^{oct}$) interstitial site is found to be more stable. Li at oxygen site behaves as a donor; however, it is not stable compared to $Li_i$ and Li at Zn site ($Li_{Zn}$). While the donor-type $Li_i$ is stable at Zn-rich and equilibrium conditions, the acceptor-type $Li_{Zn}$ becomes stable at oxygen-rich conditions (i.e., above 62% of oxygen partial pressure). The *s*-electrons of $Li_i$ is energetically well dispersed compared to that of $Li_{Zn}$ which is one of the reasons for more stability of $Li_i$. As $Li_{Zn}$ in 1− state is dominant at *n*-type conditions, the holes may compensate the electrons generated by intrinsic defects and other impurities, thus increasing the resistivity of the sample at *n*-type condition. The calculated vibrational frequencies indicate that $Li_{Zn}$ has almost similar bond-strengths along *c* and perpendicular to *c* directions. Moreover, the hybrid functional calculations indicate that $Li_{Zn}$ is a deep acceptor with the defect level at 0.74 eV above valence band maximum.

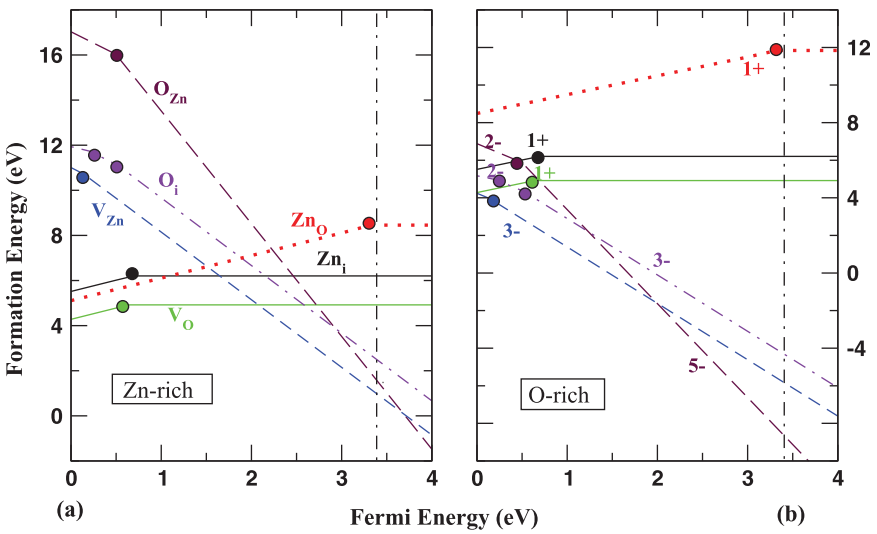


FIG. 6. Formation energy of defect complexes formed between $Li_{Zn}$ and intrinsic defects under (a) Zn-rich and (b) O-rich conditions. The dots indicate charge-transition points and the charge states are given on the illustration.

We have considered Li-impurity pairs in ZnO, viz., $2Li_i$, $2Li_{Zn}$, and $Li_i + Li_{Zn}$. While the double-donor $2Li_i$ is stable only at extreme Zn-rich condition, the double-acceptor $Li_{Zn}$ pair is stable at extreme O-rich condition. However, the $(Li_i + Li_{Zn})$ which is stable in neutral state is dominant in equilibrium condition. The complexes formed between Li-impurities and intrinsic defects are also considered and we found that the $Li_i$+intrinsic-defect complexes are more predominant than $Li_{Zn}$+intrinsic-defect complexes. The $Li_i$ +intrinsic-defect complexes are stable in donor states and have reasonable binding energies under both Zn-rich and O-rich conditions, which could cause difficulty in obtaining *p*-type conductivity in Li-doped ZnO. Among the $Li_{Zn}$ +intrinsic-defect complexes considered, the donor-type $(Li_{Zn} + V_O)$ is stable under Zn-rich condition and acceptor-type $(Li_{Zn} + V_{Zn})$ is stable under O-rich condition. Even though, these complexes are lower in energy than the compensating $Li_i + Li_{Zn}$ in respective conditions, their binding energies are very much low compared to that of $Li_i + Li_{Zn}$. In conclusion, the present study suggests that the holes generated by Li-doping in ZnO could be compensated by the intrinsic defects in the host lattice.

## ACKNOWLEDGMENTS

The authors are grateful to the Research Council of Norway for financial support and computing time on the Norwegian supercomputer facilities.

[1]S. Baruah and J. Dutta, Sci. Technol. Adv. Mater. **10**, 013001 (2009).
[2]Dhananjay, J. Nagaraj, P. R. Choudhary, and S. B. Krupanidhi, J. Phys. D: Appl. Phys. **39**, 2664 (2006).
[3]J. L. Lyons, A. Janotti, and C. G. van de Walle, Appl. Phys. Lett. **95**, 252105 (2009).
[4]E. V. Monokhov, A. Y. Kuznetsov, and B. G. Svensson, J. Phys. D: Appl. Phys. **42**, 153001 (2009).
[5]J. G. Lu, Y. Z. Zhang, Z. Z. Ye, Y. J. Zeng, H. P. He, L. P. Zhu, J. Y. Huang, L. Wang, J. Yuan, B. H. Zhao, and X. H. Li, Appl. Phys. Lett. **89**, 112113 (2003).
[6]C. H. Park, S. B. Zhang, and S.-H. Wei, Phys. Rev. B **66**, 073202 (2002).
[7]D. Y. Wang, J. Zhou, and G. Liu, J. Alloys Compd. **481**, 802 (2009).
[8]A. Onodera, N. Tamaki, Y. Kawamura, T. Sawada, and H. Yamashita, Jpn. J. Appl. Phys. **35**, 5160 (1996).
[9]A. Onodera, K. Yoshio, H. Satoh, H. Yamashita, and N. Sakagami, Jpn. J. Appl. Phys. **37**, 5315 (1998).
[10]T. Nagata, T. Shimura, Y. Nakano, A. Ashida, N. Fujimura, and T. Ito, Jpn. J. Appl. Phys. **40**, 5615 (2001).
[11]Y. J. Zeng, Z. Z. Ye, W. Z. Xu, D. Y. Li, J. G. Lu, L. P. Zhu, and B. H. Zhao, Appl. Phys. Lett. **88**, 062107 (2006).
[12]Y. J. Zeng, Z. Z. Ye, W. Z. Xu, L. L. Chen, D. Y.- Li, L. P. Zhu, B. H. Zhao, and Y.-L. Hu, J. Cryst. Growth **283**, 180 (2005).
[13]X. H. Wang, B. Yao, Z. Z. Zhang, B. H. Li, Z. P. Wei, D. Z. Shen, Y. M. Lu, and X. W. Fan, Semicond. Sci. Technol. **21**, 494 (2006).
[14]B. Xiao, Z. Ye, Y. Zhang, Y. Zeng, L. Zhu, and B. Zhao, Appl. Surf. Sci. **253**, 895 (2006).
[15]J.-R. Duclere, M. Novotny, A. Meaney, R. O'Haire, E. McGlynn, M. O. Henry, and J.-P. Mosnier, Superlattices Microstruct. **38**, 397 (2005).
[16]X. S. Wang, Z. C. Wu, J. F. Webb, and Z. G. Liu, Appl. Phys. A **77**, 561 (2003).
[17]A. H. Salama and F. F. Hammad, J. Mater. Sci. Technol. **25**, 314 (2009).
[18]S. Chawla, K. Jeyanthi, and R. K. Kotnala, Phys. Rev. B **79**, 125204 (2009).
[19]M. H. F. Sluiter, Y. Kawazoe, P. Sharma, A. Inoue, A. R. Raju, C. Rout, and U. V. Waghmare, Phys. Rev. Lett. **94**, 187204 (2005).
[20]E. C. Lee and K. J. Chang, Phys. Rev. B **70**, 115210 (2004).
[21]W.-J. Lee, J. Kang, and K. J. Chang, J. Korean Phys. Soc. **53**, 196 (2008).
[22]E.-C. Lee and K. J. Chang, Physica B **376–377**, 707 (2006).
[23]M. G. Wardle, J. P. Goss, and P. R. Briddon, Phys. Rev. B **71**, 155205 (2005).
[24]Y. Imai and A. Watanabe, J. Mater. Sci.: Mater. Electron. **15**, 743 (2004).
[25]N. R. Aghamalyan, E. K. Goulanian, R. K. Hovsepyan, E. S. Vardanyan, and A. F. Zerrouk, Phys. Status Solidi A **199**, 425 (2003).
[26]T. Yamamoto and H. K.-Yoshida, J. Cryst. Growth **214/215**, 552 (2000).
[27]T. Yamamota, Jpn. J. Appl. Phys. **42**, L514 (2003).
[28]R. Schifano, E. V. Monakhov, L. Vines, B. G. Svensson, W. Mtangi, and F. D. Auret, J. Appl. Phys. **106**, 043706 (2009).
[29]P. E. Blöchl, Phys. Rev. B **50**, 17953 (1994).
[30]G. Kresse and J. Furthmuller, Comput. Mater. Sci. **6**, 15 (1996).
[31]J. P. Perdew, S. Burke, and M. Ernzerhof, Phys. Rev. Lett. **77**, 3865 (1996).
[32]J. Heyd, G. E. Scuseria, and M. Ernzerhof, J. Chem. Phys. **118**, 8207 (2003); **124**, 219906 (2006).
[33]F. Oba, A. Togo *et al.*, Phys. Rev. B **77**, 245202 (2008).
[34]A. Janotti and C. G. Van de Walle, Appl. Phys. Lett. **87**, 122102 (2005).
[35]R. Vidya, P. Ravindran, H. Fjellvåg, B. G. Svensson, E. Monokhov, M. Ganchenkova, and R. M. Nieminen, Phys. Rev. B **83**, 045206 (2011).
[36]P. Ravindran, A. Kjekshus, H. Fjellvåg, P. Puschnig, C. Ambrosch-Draxl, L. Nordström, and B. Johansson, Phys. Rev. B **67**, 104507 (2003).
[37]C. G. Van de Walle, Phys. Rev. Lett. **85**, 1012 (2000).
[38]T. M. Børseth, B. G. Svensson, A. Y. Kuznetsov, P. Klason, O. X. Zhao, and M. Willander, Appl. Phys. Lett. **89**, 262112 (2006).
[39]H. Q. Ni, Y. F. Lu. Z. Y. Liu, H. Qiu, W. J. Wang, Z. M. Ren. S. K. Chow, and Y. X. Jie, Appl. Phys. Lett. **79**, 812 (2001).
[40]S. Lany and A. Zunger, Phys. Rev. B **80**, 085202 (2009).
[41]M.-H. Du and S. B. Zhang, Phys. Rev. B **80**, 115217 (2009).
[42]A. Carvalho, A. Alkauskas, A. Pasquarello, A. K. Tagantsev, and N. Setter, Phys. Rev. B **80**, 195205 (2009).
[43]B. K. Meyer, H. Alves, D. M. Hofmann, W. Kriegseis, D. Forster, F. Bertram, J. Christen, A. Hoffmann, M. Straßburg, M. Dworzak, U. Haboeck, and A. V. Rodina, Phys. Status Solidi B **241**, 231 (2004).
[44]C. Rauch, W. Gehlhoff, M. R. Wagner, E. Malguth, G. Callsen, R. Kirste, B. Salameh, A. Hoffmann, S. Polarz, Y. Aksu, and M. Driess, J. Appl. Phys. **107**, 024311 (2010).
[45]A. F. Kohan, G. Ceder, D. Morgan, and C. G. Van de Walle, Phys. Rev. B **61**, 15019 (2000).
[46]S. B. Zhang, S.-H. Wei, and A. Zunger, Phys. Rev. B **63**, 075205 (2001).
[47]T. Nakagawa, I. Sakaguchi, K. Matsunaga, T. Yamamoto, H. Haneda, and Y. Ikuhara, Nucl. Inst. Methods Phys. Res. B **232**, 343 (2005).
[48]H. Kwak, M. L. Tiago, T.-L. Chan, and J. R. Chelikowsky, Chem. Phys. Lett. **454**, 338 (2008).
[49]S. B. Orlinskii, J. Schmidt, P. G. Baranov, D. M. Hofmann, C. M. Donega, and A. Meijerink, Phys. Rev. Lett. **92**, 047603 (2004).
[50]S. B. Orlinskii, J. Schmidt, E. J. J. Groenen, P. G. Baranov, C. M. Donega, and A. Meijerink, Phys. Rev. Lett. **94**, 097602 (2005).
[51]C. D. Pemmaraju, T. Archer, R. Hanafin, and S. Sanvito, J. Magn. Magn. Mater. **316**, e185 (2007).
[52]T. Yamamoto and H. K.-Yoshida, Physica **302–303**, 155 (2001).
[53]G.-Y. Huang, C.-Y. Wang, and J.-T. Wang, J. Phys.: Condens. Matter **21**, 345802 (2009).